Materials Research Proceedings 41 (2024) 983-988 https://doi.org/10.21741/9781644903131-108

Molecular dynamics simulation for determining dislocation strengthening coefficient in BCC iron

MIYAZAWA Naoki[1,a *] and HAMA Takayuki[1,b]

[1] Graduate School of Energy Science, Kyoto University, Kyoto 606-8501, Japan

[a] miyazawa.naoki.3n@kyoto-u.ac.jp, [b]hama@energy.kyoto-u.ac.jp

Keywords: Molecular Dynamics Simulation, Crystal-Plasticity Analysis, Dislocation Strengthening

Abstract. Crystal plasticity models are promising numerical analysis methods for predicting and evaluating material forming processes. In crystal plasticity analyses, the dislocation density model, often based on the Bailey-Hirsch equation, is employed to represent the work hardening behavior of metallic materials. The dislocation strengthening coefficient is a proportional factor between the square root of dislocation density with the slip resistance. Therefore, the appropriate determination of the dislocation strengthening coefficient is crucial to perform reliable material forming analyses using crystal plasticity models. Previously, dislocation strengthening coefficients have been determined using dislocation dynamics simulations. However, dislocation dynamics simulations cannot accurately account for elastic anisotropy due to its computational cost. To address this limitation, we conducted molecular dynamics simulations to determine dislocation strengthening coefficient in bcc iron. Molecular dynamics simulations of dislocation-dislocation interaction analysis can be expected to determine the dislocation strengthening coefficient accurately, including the effects of elastic anisotropy of metallic materials.

Introduction

Crystal plasticity finite-element methods (CPFEM) are promising numerical tools to predict metallic material forming processes accurately. To accurately predict deformation processes through CPFEM, the selection of a work hardening model and the determination of relevant parameters are crucial. The dislocation density model is a work hardening model based on the Bailey-Hirsch equation, where slip resistance is assumed to be proportional to the square root of dislocation density. When explicitly considering interactions between different slip systems of α and β, the dislocation density model can be written, for example, as follows:

$$\tau_C^{(\alpha)} = \tau_Y^{(\alpha)} + \mu|\boldsymbol{b}|\sqrt{\textstyle\sum_\beta d_{\alpha\beta}\rho_\beta}, \quad (1)$$

where τ_C, τ_Y, μ, $\boldsymbol{b}$, ρ and $d_{\alpha\beta}$ are slip resistance, reference shear stress, burgers vector, shear modulus, dislocation density and dislocation strengthening coefficient matrix, respectively.

Since experimental determination of $d_{\alpha\beta}$ is difficult, dislocation dynamics (DD) simulations have been previously used to determine dislocation strengthening coefficients [1]. DD simulation is a numerical simulation method to model the dynamics of dislocation motion based on the continuum elastic theory. By precisely modeling dislocation network, DD simulation can simulate the work-hardening behavior of a metallic material in a depiction close to real materials. However, accuracy of DD simulation may be questionable because elastic anisotropy is not adequately considered due to its computational cost. For example, when the angles between slip planes are the same, the dislocation strengthening coefficients determined by DD simulation absolutely show the same value, even in the case of different combinations of slip systems. Therefore, simply introducing the dislocation strengthening coefficients obtained from DD into CPFEM does not

Materials Research Proceedings 41 (2024) 983-988 https://doi.org/10.21741/9781644903131-108

ensure the accurate reproduction of stress-strain curve of real materials, even though they are presumed to have some validity.

Molecular dynamics (MD) simulations numerically solve the equations of motion for individual atoms constituting a material. It can accurately predict the plastic deformation behavior of metallic materials, considering the elastic anisotropy of the material within the limitation of the accuracy of interatomic potential function. Previous MD studies have investigated dislocation-dislocation interactions on fcc [2] and bcc [3] metals. While these studies extensively examined the dislocation-dislocation interactions within a specific combination of slip systems, limited MD researches have been conducted on the differences of slip resistance between various combinations of slip systems. As a result, the dislocation strengthening coefficients determined by MD simulations are largely unknown.

In the present study, MD simulations were conducted to determine the dislocation strengthening coefficients in bcc Fe, including the effect of elastic anisotropy. Dislocation-dislocation interactions were investigated for different combinations of slip systems, including {110}/{110}, {112}/{112} and {112}/{110} as active/forest dislocation interactions. The resulting dislocation reactions due to dislocation interactions were discussed in detail. The dislocation strengthening coefficients were calculated based on the critical stress ratio of dislocation reactions. Results of MD simulations were compared with previous DD simulations to investigate the changes in dislocation strengthening coefficients resulting from the influence of elastic anisotropy.

Computational Methods

All MD simulations were performed using classical MD code LAMMPS [4] developed in Sandia National Laboratories. A computational cell of a single-crystalline bcc iron is shown in Fig. 1. After considering the limitations of MD simulations regarding the number of atoms they can handle, the simulation cell was set up with a single screw dislocation as the active slip and a single edge dislocation as the forest dislocation. The number of atoms included in the cell was about 6 million. The initial atomic coordinates around dislocations were determined based on the elastic solution for the displacement field of the dislocation within anisotropic elastic media [5]. The employed interatomic potential was the Embedded-Atom-Method (EAM) potential of Chamati et al. [6], where the potential can accurately predict the Peierls stress in bcc Fe. The MD simulations were performed under constant number of particles, volume and temperature (NVT) ensemble. The timestep of time integration was 1 fs and the temperature was fixed at 5 K throughout simulations. The fixed boundary condition was applied in the *z*-direction and free boundary condition was applied in the *x*- and *y*-directions. Note that the periodic boundary conditions cannot be applied to all directions because of the discontinuity in displacement fields of dislocations within periodic boundary.

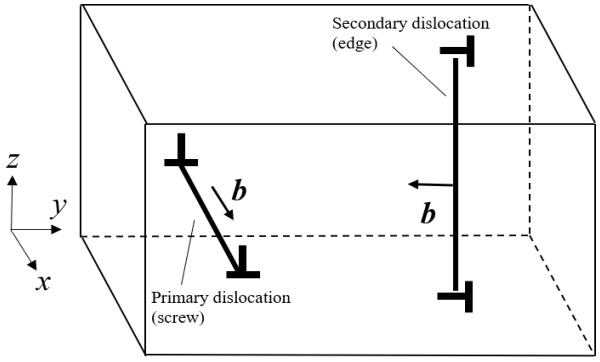

Fig.1 Simulation cell used in the present study.

Energetically stable atomistic configuration was achieved through energy minimization with a conjugate gradient method and 100 ps-relaxation simulations. To activate the glide of active screw dislocation, shear strain at a constant strain rate (=10^7 s^{-1}) was applied to the cell by introducing a constant velocity displacement in the *x*-direction of the upper outermost *z*-layer. According to the previous MD study [3], below 10^7 s^{-1} strain rate condition, the dislocation motion velocity has been reported not to exceed the speed of sound. The dislocation reactions as a result of interactions

between active screw and forest edge dislocations were investigated, where the combination of active/forest dislocations were {110}/{110}, {112}/{112} and {112}/{110} slip systems, respectively (Table 1). In dislocation analysis, there are two processes: immobile dislocation formation and dislocation annihilation. Among them, this study specifically investigated immobile dislocation reactions. The dislocation strengthening coefficients were calculated as the critical stress ratio of dislocation reactions for different dislocation reactions.

Table 1 The combinations of slip systems considered in the present study.

	Active/forest dislocation slip system
{110} screw/{110} edge	[111](0)/[1](110), [111](01)/[1](101), [111](01)/[1](01), [111](01)/[1](110)
{112} screw/{112} edge	[111](11)/[1](211), [111](11)/[1](112), [111](11)/[1](12)
{112} screw/{110} edge	[111](12)/[111](01), [1](121)/[111](01), [11](1)/[111](01), [1](2)/[111](01), [1](211)/[111](01)

Results

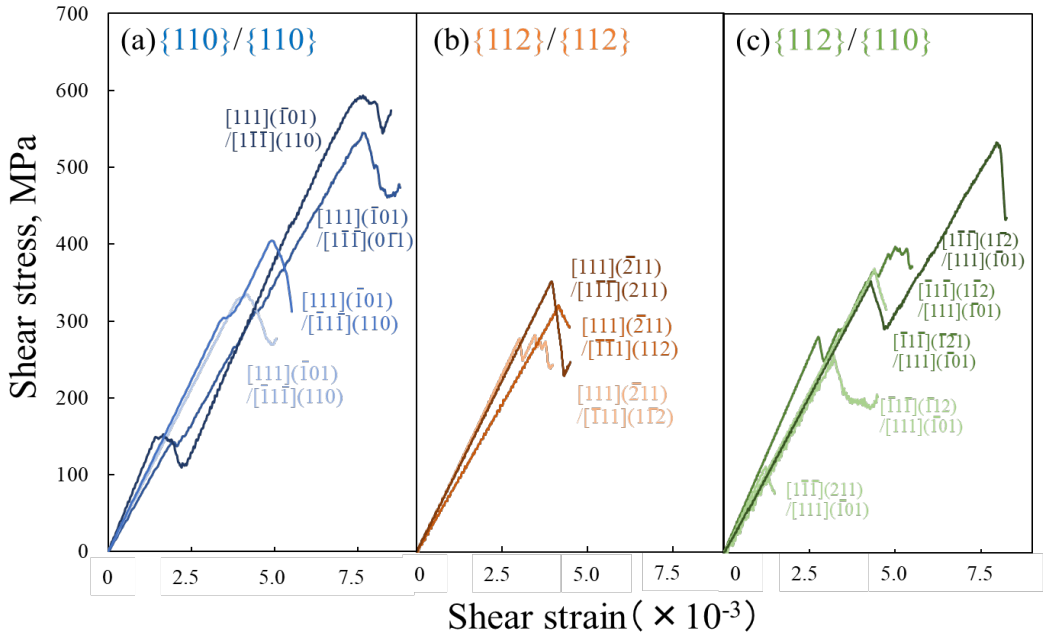

Fig. 2 Stress-strain curves for (a) {110}/{110}, (b) {112}/{112} and (c) {112}/{110} interactions, respectively.

The stress-strain curves for all considered combinations of slip systems in this study are shown in Fig. 2. Unlike the stress-strain curves of real bulk pure-Fe, the curves in the present study did not show a flow curve, but exhibited linear increase followed by reaching peak and subsequent decrease. In addition, the strain until reaching the peak is very small. This is attributed to the limited number of dislocations within the computational cell, and therefore, dislocation interaction frequency was limited in the present study. Variations of critical stresses of dislocation-dislocation interactions were observed depending on different combinations of slip systems. The flow stresses of MD shear simulations were much higher than those of experimental values of pure bcc Fe, because the dislocation density of the present study was high value of about 10^{15} m^{-3}. The

{110}/{110} interactions (Fig.2a) tend to exhibit higher critical stresses compared to {112}/{112} (Fig.2b) and {112}/{110} interactions (Fig.2c).

Fig.3 shows the changes in dislocation configuration during a dislocation reaction. When shear strain was applied to the computational cell, the active screw dislocation approached to the forest edge dislocation (Fig.3a) and they underwent crossover event (Fig.3b). The active screw dislocation cross-slipped and ***a***[001] immobile dislocation was formed (Fig.3c). The corresponding dislocation reaction can be written as follows:

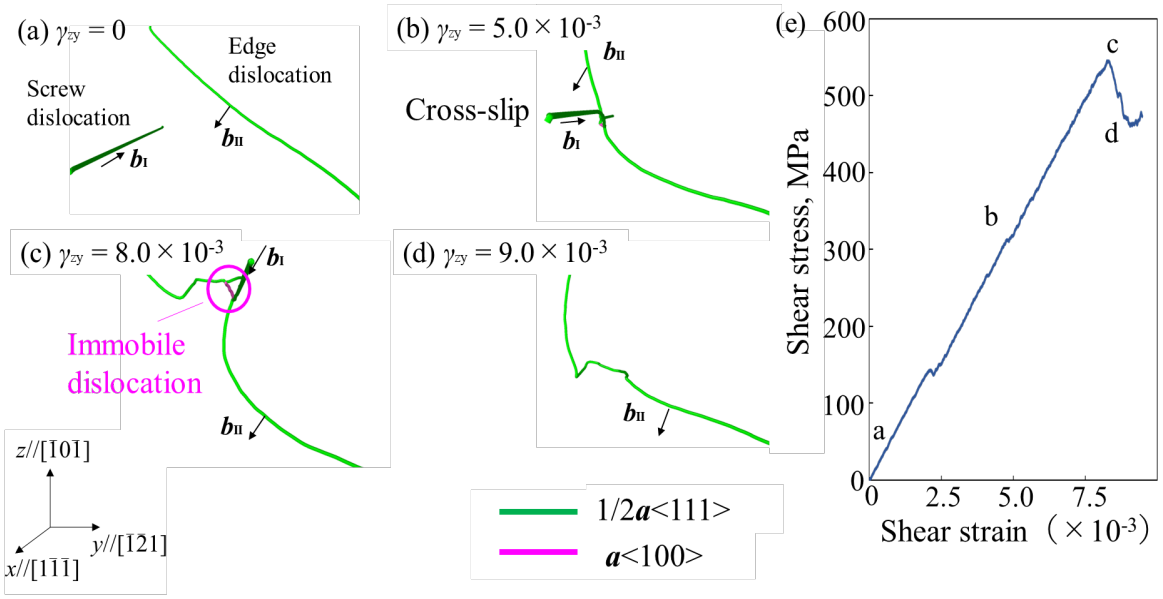

Fig. 3 Dislocation configuration change during dislocation reaction when applied shear strain γ_{zy} is (a) 0.0, (b) 5.0×10^{-3}, (c) 8.0×10^{-3} and (d) 9.0×10^{-3}, respectively. (e) Comparison of dislocation configuration with stress-strain curve.

$$\boldsymbol{a}[111] + \boldsymbol{a}[1] \rightarrow \boldsymbol{a}[001]. \quad (2)$$

The immobile dislocation ***a***[001] acts as a strong obstacle to active slip, resulting in work hardening from a macroscopic perspective. By continuous cross-slip of active screw dislocations, the positions of formed immobile dislocations shifted within the cell as a result of the repeated process of localized detachment from and formation of immobile dislocations. As the shear strain increased, the active screw dislocation completely escaped from the immobile dislocation and the forest edge dislocation was left within the simulation box (Fig.3d).

Fig.3e shows the comparison of the changes in dislocation configurations and corresponding stress-strain curve. As seen from the figure, the critical stress of the dislocation reaction was achieved when just before the active screw dislocation escaped from the immobile dislocation. Therefore, in this study, the critical stress can be mainly governed by the formation and detachment stress of immobile dislocations. In all combinations of slip systems, the dislocation reactions themselves were the same as Eq.2, but the length and the line directions of the formed immobile dislocations were different depending on combinations of slip systems.

Discussion

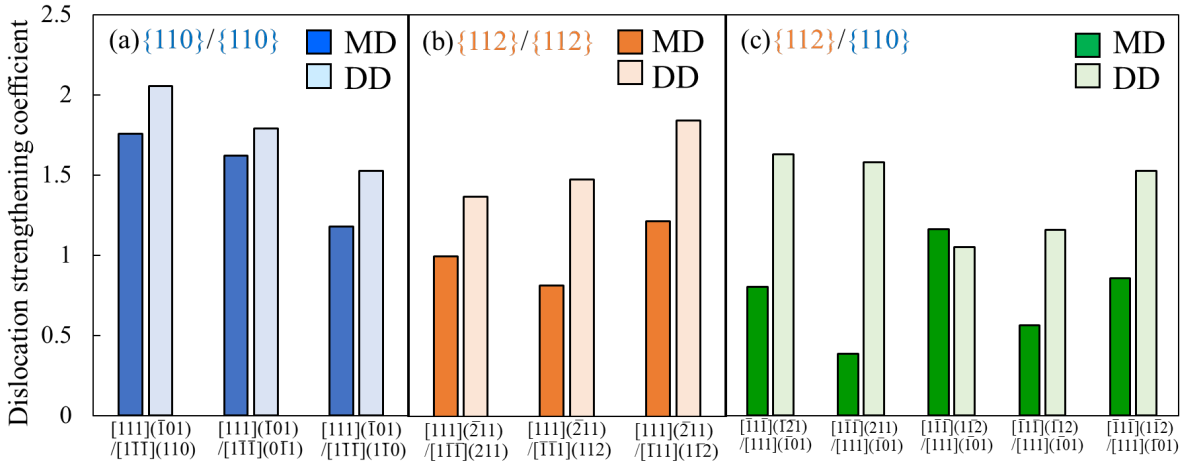

Fig. 4 Dislocation strengthening coefficients calculated by MD and their comparison with previous DD simulations for (a) {110}/{110}, (b) {112}/{112} and (c) {112}/{110} interactions, respectively. The values are compared with [111](01)/[11](110) interaction.

Fig.4 shows dislocation strengthening coefficients obtained from MD (present study) and previous DD simulations. For {110}/{110} interactions (Fig. 4a), the coefficients obtained from MD simulations were slightly smaller than DD results, but they almost showed the same values. This suggests the potential reliability of MD simulations in predicting dislocation strengthening coefficients. As discussed in results section, the critical stresses in MD simulations were mainly determined by formation and detachment stress of immobile dislocations. Thus, the dislocation strengthening coefficient can be predominantly determined by the strength of an immobile dislocation as an obstacle. The slight differences observed between the MD and DD results are attributable to the utilization of large dislocation density (=about 10^{15}m^{-3}) and high strain rate (=10^{7}s^{-1}) in the current MD simulations. However, these effects were expected to be nearly canceled since dislocation strengthening coefficients are determined based on the ratio of critical stresses. For {112}/{112} interactions (Fig. 4b), MD and DD results also showed similar values, but the magnitudes of the differences were larger compared to the {110}/{110} interactions. In contrast, for {112}/{110} interactions (Fig. 4c), there were some variations in the values of MD and DD simulations.

The reason for the discrepancies in results between the MD and DD simulations when considering {112} slip systems can be their treatment of elastic anisotropy. In the DD simulation, the dislocation motion is numerically analyzed under the assumption of elastic isotropy. Therefore, shear on {110} and {112} shows the same tendency. In the MD simulation, however, elastic response on {110} and {112} shear is different, where shear modulus μ of {112} system is about 13% smaller than {110} system in the present MD simulation. In classical elastic continuum theory, the orientation-dependent dislocation line energy per unit length E can be written as follows [7]:

$$E = \frac{\mu b^2(1-\nu\cos^2\beta_{dis})}{4\pi(1-\nu)} ln(\frac{R}{b}), \quad (3)$$

where the angle β_{dis} defines the geometrical character of the dislocation segment. In this equation, materials properties are represented by shear modulus μ and Poisson's ratio ν, indicating that the difference of μ is crucial to determine critical stress of dislocation interactions.

Note that the present study just focused on calculating the dislocation strengthening coefficients and comparing the MD results to DD results. The MD results obtained in the present study does

not immediately enhance the accuracy of stress-strain curve prediction in real materials. However, our finding, significant differences between MD and DD in the coefficients of {112}/{110} interactions due to elastic anisotropy is meaningful. To understand the effect of elastic anisotropy on work hardening of materials more deeply, macroscopic materials deformation analysis such as CPFEM is necessary. The comparison with real materials and the quantitative validation of MD results are future work.

Summary

In summary, MD simulations were performed to determine the dislocation strengthening coefficients in bcc Fe. The interaction between active screw dislocation and forest edge dislocation was investigated using MD shear test simulations. A immobile dislocation ***a***[001] was formed as a result of dislocation reaction with the activation of cross-slip of the screw dislocation. The peak stress in stress-strain curve was obtained just before the active dislocation escaped from the formed immobile dislocation. The critical stresses in the dislocation reactions varied depending on the combinations of slip systems between active and forest dislocations. For {110}/{110} interactions, the calculated dislocation strengthening coefficients showed values slightly smaller but closely aligned with the previous DD values. Thus, MD simulations can be reliable to determine dislocation strengthening coefficients. Similarly, MD and DD values exhibited close values, but the differences were larger in {112}/{112} than in {110}/{110} interactions. In contrast, for {112}/{110} interactions, some variations in the quantitative magnitude of dislocation strengthening coefficients was observed between MD and DD simulations. The differences in values, particularly in cases involving {112} slip systems, are attributable to the treatment of elastic anisotropy in both computational methods because the stress required for dislocation reaction is largely dependent on the shear modulus. In MD simulation, anisotropic elasticity is considered within the range of interatomic potential reliability, while isotropic elasticity is considered in DD simulation due to its computational cost. The results of the MD simulations in the present study have the potential to enhance the prediction accuracy of work hardening in CPFEM simulation through the consideration of elastic anisotropy.

References

[1] R. Madec and L. P. Kubin, Dislocation strengthening in FCC metals and in BCC metals at high temperatures, Acta Mater. 126 (2017) 166-173. https://doi.org/10.1016/j.actamat.2016.12.040

[2] S. J. Zhou, D. L. Preston, P. S. Lomdahl and D. M. Beazley, Large-scale molecular dynamics simulations of dislocation interaction in copper, Science 279 (1998) 1525-1527. https://doi.org/10.1126/science.279.5356.1525

[3] S. M. Hafez Haghighat, R. Scha¨ublin and D. Raabe, Atomistic simulation of the a_0 <100> binary junction formation and its unzipping in body-centered cubic iron, Acta Mater. 64 (2014) 24-32. https://doi.org/10.1016/j.actamat.2013.11.037

[4] S. Plimpton, Fast parallel algorithms for short-range molecular dynamics, J. Compt. Phys. 117 (1995) 1-19. https://doi.org/10.1006/jcph.1995.1039

[5] D. J. Bacon, D. M. Barrett and R. O. Scattergood, Anisotropic continuum theory of lattice defects, Prog. Mater. Sci. 23 (1979) 51-262. https://doi.org/10.1016/0079-6425(80)90007-9

[6] H. Chamati, N. I. Papanicolaou, Y. Mishin and D. A. Papaconstantopolous, Embedded-atom potential for Fe and its application to self-diffusion on Fe(100), Surf. Sci. 600 (2006) 1793-1803. https://doi.org/10.1016/j.susc.2006.02.010

[7] G. de Wit and J.S. Koehler, Interactions of dislocations with an applied stress in anisotropic crystals, Phys. Rev. B, 116 (1959) 1113–1120. https://doi.org/10.1103/PhysRev.116.1113